

Mixed Convection Flow and Heat Transfer of Two Rotating Cylinders in a Trapezoidal Enclosure Filled with Porous Medium

Bader Alshuraiaan

Mechanical Engineering Department, Kuwait University, Safat 13060, Kuwait

Corresponding Author Email: alshuraiaan@yahoo.com



<https://doi.org/10.18280/ijht.400619>

ABSTRACT

Received: 30 April 2022

Accepted: 16 December 2022

Keywords:

mixed convection, porous medium, rotating cylinders, trapezoidal cavity, two cylinders

The goal of this research is to investigate numerically mixed convection flow and heat transfer characteristics from two rotating cylinders in a trapezoidal enclosure filled with porous material for a variety of factors including rotation speed and direction, Richardson number, and the location of the cylinders. The results of this presentation were checked against accessible data and determined to be very similar. The heat transmission properties within the trapezoid were found to be substantially dependent on the Richardson number, speed, and direction of the spinning cylinders, as well as the location of the cylinders according to the findings of this study. Furthermore, it was discovered that the CW-CW casing produced more heat transfer as compared to the CCW-CW scenario for various Richardson numbers when the cylinders placed vertically. Furthermore, this research revealed that, for higher Richardson values, the rotation speed has no effect on the heat transfer increase inside the trapezoidal enclosure. The effect of the cylinders' location on the average Nusselt number was also studied in this investigation. It was found the placing the cylinders in the vertical direction produced higher heat transfer compared with horizontal location for a trapezoid heated from below.

1. INTRODUCTION

Due to its importance in various applications such as nuclear reactors, chemical catalytic reactors, petroleum reservoirs, solar power, microelectronics, and ground hydrology, mixed convection flow and heat transfer in porous medium have sparked a lot of attention in the literature [1-7]. Free convection in cavities with single and multiple cylinders has been widely investigated both computationally and experimentally [8-14]. Park et al. [8] investigated numerically free convection in a chamber with two hot and cold cylinders positioned vertically at different locations. Their findings revealed that the Nusselt number computations were influenced by the cylinder placements. Park et al. [9] looked at the free convection inside the cavity generated by temperature differences in the cavity walls and inner hot cylinders. Their findings demonstrated the considerable impact of enclosing cylinders on heat transfer enhancement.

In the literature, the effect of revolving cylinders in enclosures has received less attention [15-17]. Khanafer et al. [17] investigated the influence of two revolving cylinders in a cavity in the absence of a porous medium numerically for a number of key factors. The heat transfer enhancement inside the cavity was shown to be substantially dependent on the cylinder speed of rotation as well as the Richardson number, according to their findings. Selimefendigil and Oztop [16] investigated numerically flow and heat transport in a lid-driven cavity comprising two spinning cylinders using the finite element method. In that investigation, ferrofluid was used. Their studies revealed that the rate of heat transmission increased as the temperature rose. In an enclosure with two cold-wavy vertical sides and insulated bottom-to-top walls,

Majdi et al. [18] analyzed numerically the convection heat transfer from a heated cylinder. A porous medium is present in the left side of the domain and a nanofluid is present inside the cavity. Their findings demonstrate how the presence of porous media and nanofluid improves the heat transmission process.

The effect of two spinning cylinders on flow and heat transfer in a trapezoidal enclosure has never been examined before, as evidenced by the aforementioned reference. The goal of this study is to calculate the effects of changing several relevant parameters such as Richardson number, cylinder speed and direction, and location on the average Nusselt number, streamlines, and isotherms.

2. MATHEMATICAL FORMULATION

Figure 1 depicts the configuration of the problem under research in this study. In the trapezoidal container, two rotating cylinders are positioned vertically. Both cylinders' radii are considered to be equal ($r_0=0.1H$). The cylinders are supposed to rotate at an angle of ω_0 at all times. The trapezoid's fluid flow is laminar, 2D, stable, and incompressible. On the trapezoidal enclosure's walls, no slip boundary condition is enforced. The left and right walls, as well as the cylinder walls, are assumed to be adiabatic, with the bottom hot wall kept at T_h and the top wall at T_c . As a working fluid, the trapezoidal cavity is filled with air ($Pr=0.7$). The porous medium in this investigation is assumed homogenous, isotropic, and is saturated with a fluid that is in local thermodynamics equilibrium with the solid matrix. This research considers the Forchheimer-Brinkman-extended Darcy model to take into

account the effect of inertia and solid boundaries. In dimensionless form, the governing equations are as follows [19-21]:

$$\frac{\partial U}{\partial X} + \frac{\partial V}{\partial Y} = 0 \quad (1)$$

$$\begin{aligned} \frac{1}{\varepsilon^2} \left(U \frac{\partial U}{\partial X} + V \frac{\partial U}{\partial Y} \right) &= -\frac{1}{Re} \frac{\partial P}{\partial X} + \frac{\nabla^2 U}{\varepsilon Re} - \frac{U}{Re Da} \\ &\quad - \frac{C_F}{Re \sqrt{Da}} U \sqrt{U^2 + V^2} \end{aligned} \quad (2)$$

$$\begin{aligned} \frac{1}{\varepsilon^2} \left(U \frac{\partial V}{\partial X} + V \frac{\partial V}{\partial Y} \right) &= -\frac{1}{Re} \frac{\partial P}{\partial Y} + \frac{\nabla^2 V}{\varepsilon Re} - \frac{V}{Re Da} \\ &\quad - \frac{C_F}{Re \sqrt{Da}} V \sqrt{U^2 + V^2} + \frac{Gr}{Re^2} \theta \end{aligned} \quad (3)$$

$$U \frac{\partial \theta}{\partial X} + V \frac{\partial \theta}{\partial Y} = \frac{k_{eff}}{k_f} \frac{\nabla^2 \theta}{Pr Re} \quad (4)$$

where, ε is the porosity and C_F is the Forchheimer coefficient expressed by [19-21]:

$$C_F = \frac{1.75}{\sqrt{150\varepsilon^3}} \quad (5)$$

The effective thermal conductivity of the porous medium, k_{eff} , is given by:

$$k_{eff} = \varepsilon k_f + (1 - \varepsilon) k_s \quad (6)$$

The above equations were written in nondimensional form by applying the followings:

$$\begin{aligned} X = \frac{x}{H}, \quad Y = \frac{y}{H}, \quad U = \frac{u}{u_o}, \quad V = \frac{v}{u_o}, \\ \theta = \frac{(T - T_C)}{(T_H - T_C)}, \quad P = \frac{\rho H}{\rho \nu u_o} \end{aligned} \quad (7)$$

$$u_o = r_o \omega_o, \quad Re = \frac{u_o H}{\nu},$$

$$Gr = \frac{g \beta (T_H - T_C) H^3}{\nu^2}, \quad Pr = \frac{\nu}{\alpha}$$

The dimensionless boundary conditions used in this investigation are summarized as follows:

$$\text{Left and right surfaces: } U = V = \frac{\partial \theta}{\partial n} = 0 \quad (8)$$

$$\text{Top wall: } U = V = 0, \quad \theta = 0$$

$$\text{Bottom wall: } U = V = 0, \quad \theta = 1 \quad (9)$$

The boundary conditions for the cylinders are:

$$\frac{\partial \theta}{\partial n} = 0 \quad (10a)$$

$$\text{Angular velocity: } \varpi = \varpi_o \quad (10b)$$

Moreover, the average Nusselt number at the cold wall of the trapezoidal enclosure:

$$\overline{Nu} = - \int_0^1 \frac{\partial \theta}{\partial Y} \Big|_{Y=1} dX \quad (11)$$

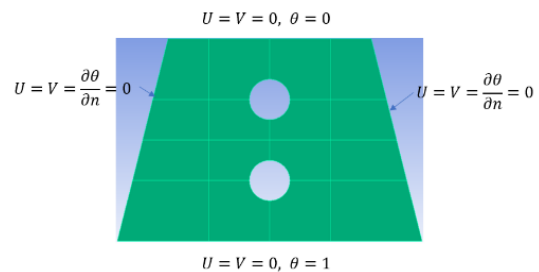


Figure 1. Schematic diagram of the problem

2.1 Numerical scheme

Galerkin-weighted residual method of the finite element method was used in this investigation. COMSOL 5.4 Multiphysics software was utilized in this investigation. A free unstructured mesh of triangular elements with fine mesh near the rotating cylinders and in the vicinity of walls were deployed to catch the rapid variations in the variables. A mesh size of 181 by 181 was found sufficient to get grid-independent results (Table 1).

Table 1. Grid-Independent analysis (Re=100, Pr=0.7, Ri=1, $\varpi=10$)

Grid Size	Average Nusselt Number
81×81	4.21
121×121	4.32
181×181	4.44
251×251	4.44

2.2 Code validation

The findings of this study were corroborated by a number of other findings. Table 2 demonstrates a strong correlation between the current findings and those of Khanafer and Aithal [22] in terms of average Nu. Furthermore, Figure 2 shows an outstanding comparison of streamlines and isotherms between the two results. Furthermore, Figure 3 demonstrates that the streamlines and isotherms of the current results and those of Khanafer and Chamkha [23] are very similar.

Table 2. Comparison of the average Nusselt in a lid-driven cavity with a rotating cylinder (Re=100, Pr=0.7, Ri=1)

Cylinder Speed (ϖ)	Present	Khanafer and Aithal [22]
1	3.64	3.64
2	3.82	3.82
3	3.94	3.95
5	4.14	4.13
10	4.44	4.46

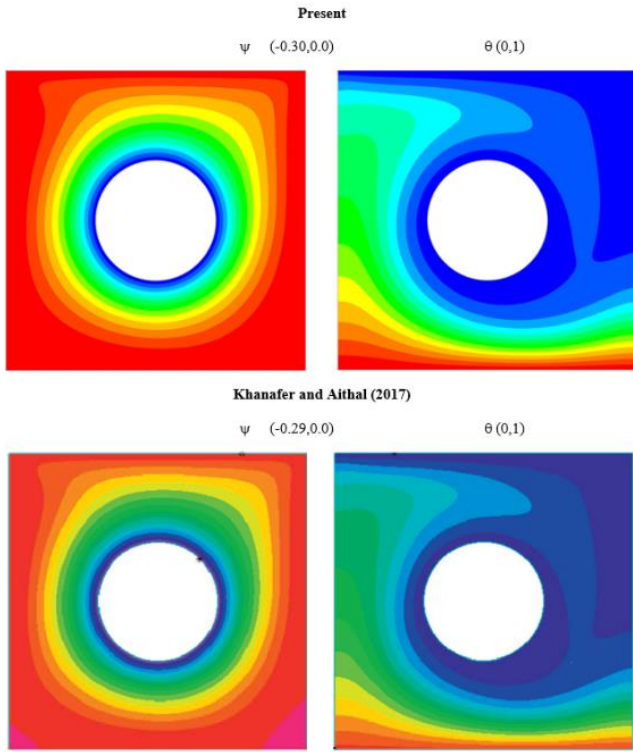


Figure 2. Comparison of the streamlines and isotherms between the current work and that of Khanafer and Aithal [22] ($Re=100$, $Pr=0.7$, $Ri=1$, $\varpi=10$)

looked at the effects of changing the Richardson number, cylinder speed, and rotation direction on streamlines, isotherms, and the average Nusselt number. Prandtl number of 0.7, Reynolds number of 100, and Darcy number of 0.01 were chosen as default values in this investigation. For a small speed of 0.5, Figures 4 and 5 show the effect of changing the Richardson number and direction of rotation on the streamlines and isotherms. Increases in the Richardson number were found to have a considerable effect on the streamline distribution around the two-rotating cylinder, as seen in Figure 4. This is caused by an increase in the cavity's velocity. Furthermore, Figure 4 clearly illustrates that the effect of rotation direction on streamline fluctuations was considerable at low Richardson number values for a modest speed of 0.5. The rotation direction of the cylinders had little effect on streamlines for large Richardson values. Figure 4 illustrates that in the CW-CW example, the major vortex is dispersed symmetrically around both cylinders, with two minor vortices near to the inclined surfaces, for a low Rayleigh number of $Ri=0.01$.

For higher Rayleigh numbers, this symmetry does not exist. At low speeds, the isotherms for the influence of Richardson number and rotation direction show identical behavior as depicted in Figure 5. The isotherms are essentially horizontal for low Richardson numbers, except near the cylinders, indicating heat transmission primarily by conduction.

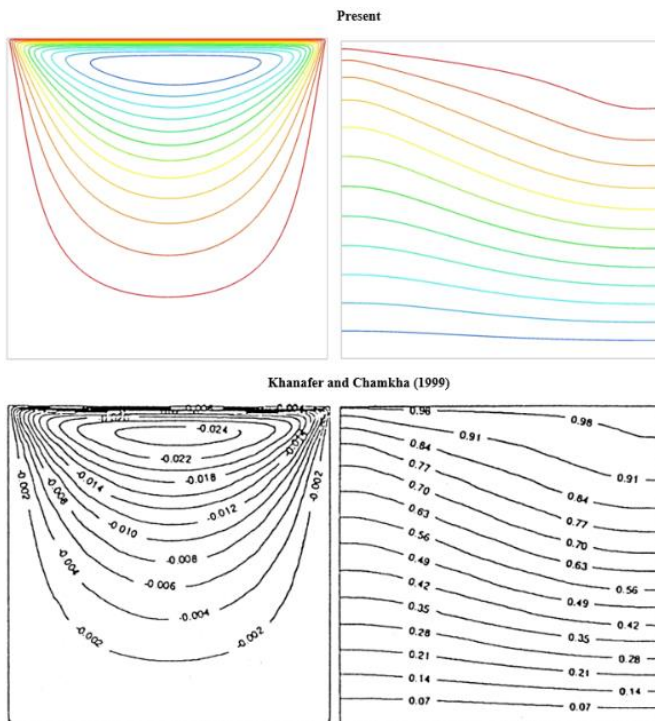


Figure 3. Comparison of streamlines and isotherms between the current results and that of Khanafer and Chamkha [23] ($Re=100$, $Ri=0.01$, $Pr=0.7$, $Da=10^{-3}$)

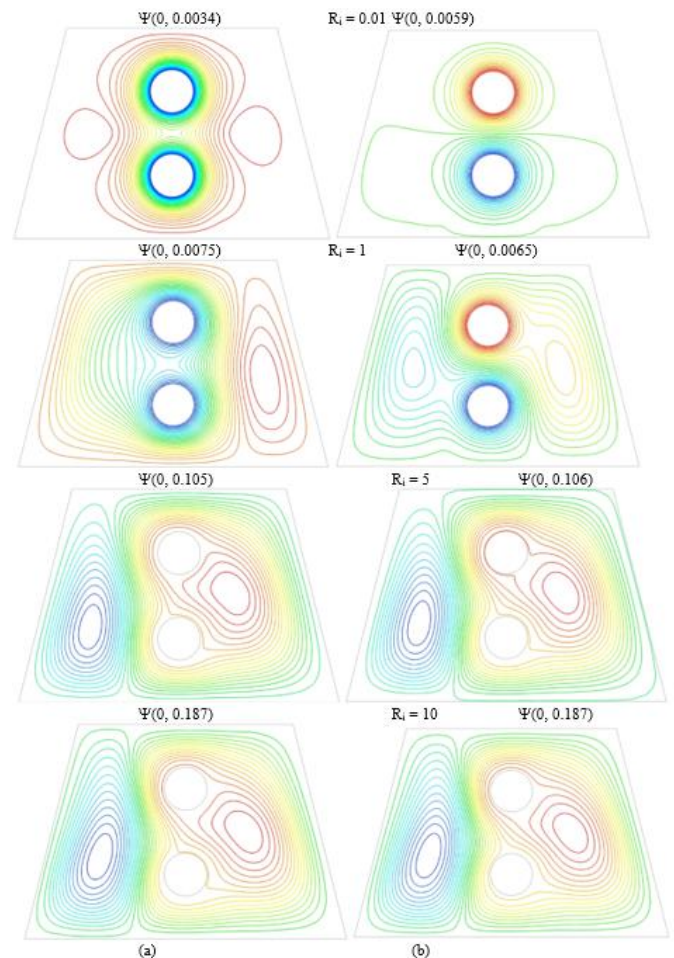


Figure 4. Comparison of the streamlines contours for different directions of the angular velocity (a) both cylinders CW and (b) top CCW and bottom cylinder CW ($Re=100$, $Da=0.01$, $\varpi=0.5$)

3. RESULTS AND DISCUSSION

Although the effect of the Darcy number has been stated by numerous writers, it was not explored in this work. This study

Natural convection gains significantly in strength as the Richardson number rises, compared to forced convection caused by revolving cylinders. The thermal boundary layer along the cavity's bottom surface thins out, increasing heat transfer dramatically. As shown in Figure 5, the effect of altering the cylinders' rotation direction has a negligible effect at low rotational speeds. This indicates that the Rayleigh number controls the heat transmission properties within the cavity.

Figures 6 and 7 show how raising the cylinder speed ($= 10$) affects the streamlines and isotherms for different Richardson numbers.

Both graphs show that the Richardson number and rotation direction have a significant impact on flow and temperature patterns. The top CCW cylinder-CW bottom cylinder scenario has higher convection intensity than both CW cylinders scenario for Richardson number smaller than one, as seen in Figure 6. However, for Rayleigh values greater than 1, the CW-CW scenario shows a considerable increase in convection activity as compared to the CCW-CW scenario.

In comparison to the CCW-CW situation, the CW-CW scenario aids the buoyancy effect. This is supported by Figure 7, which shows that the thermal boundary layers for the CW-CW scenario are thinner than those for the CCW-CW scenario, indicating better heat transfer characteristics. For various Richardson values, Figure 8 shows the effect of adjusting the angular velocity of the cylinders on heat transfer improvement. The average Nusselt number is almost constant for modest rotation speeds ($\omega=0.5$) and the Richardson number is below 1.

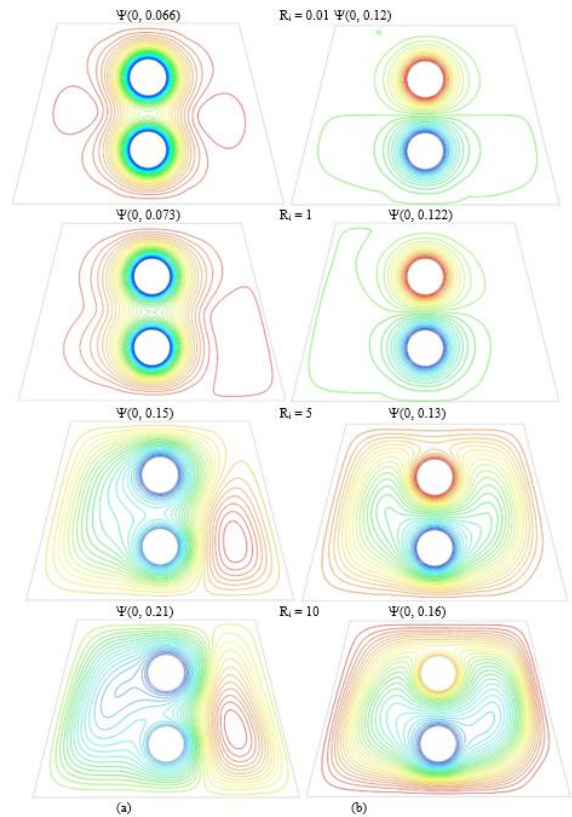


Figure 6. Comparison of the streamlines contours for different directions of the angular velocity (a) both cylinders CW and (b) top CCW and bottom cylinder CW ($Re=100$, $Da=0.01$, $\omega=10$)

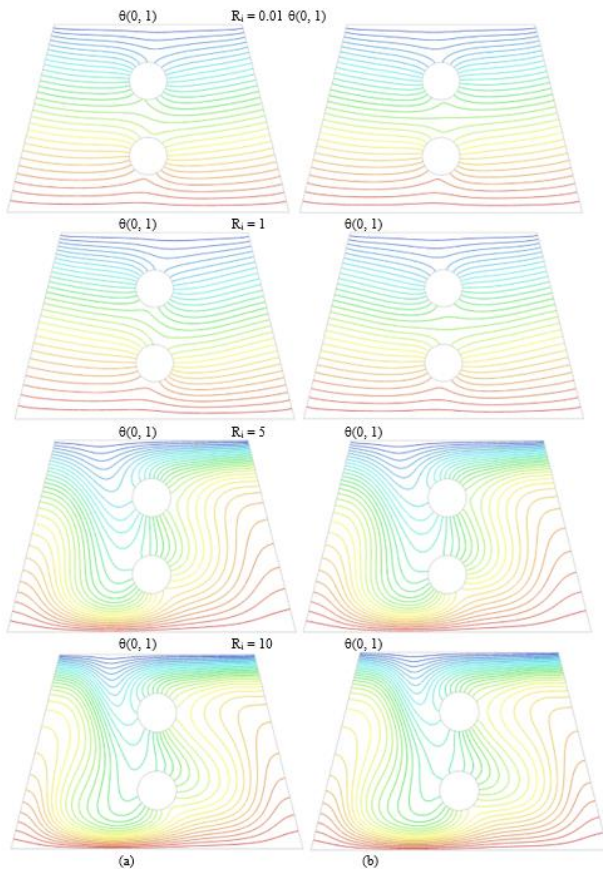


Figure 5. Comparison of the isotherms for different directions of the angular velocity (a) both cylinders CW and (b) top CCW and bottom cylinder CW ($Re=100$, $Da=0.01$, $\omega=0.5$)

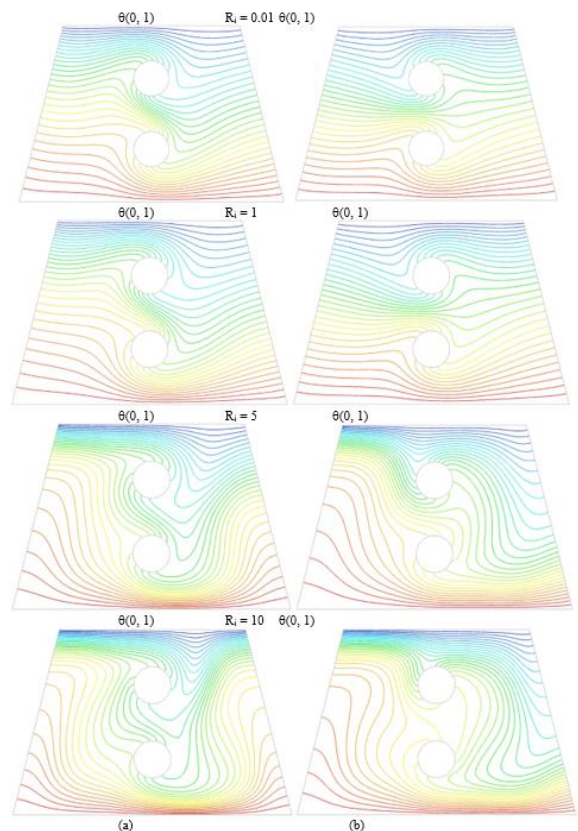


Figure 7. Comparison of the isotherms for different directions of the angular velocity (a) both cylinders CW and (b) top CCW and bottom cylinder CW ($Re=100$, $Da=0.01$, $\omega=10$)

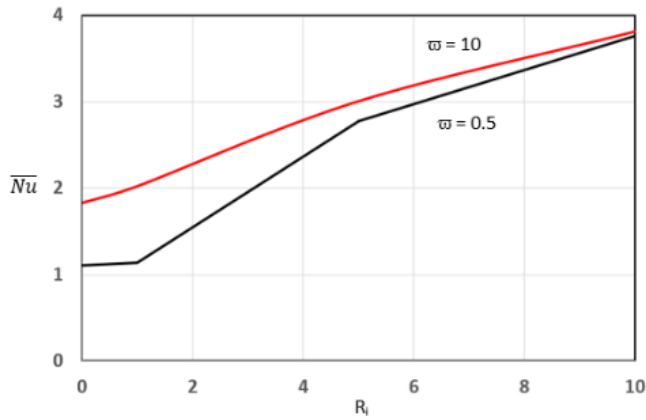


Figure 8. Effect of varying the angular velocity and Richardson number on the average Nusselt number of the top surface – both cylinders rotating clockwise ($Re=100$, $Da=0.01$)

The average Nusselt number rises for a given Richardson number. It's worth noting that, for the Richardson range of 1 to 5, the rate of growth in the average Nusselt is higher for low rotation speed compared to large rotation speed. Figure 8 shows that the rotation speed has no effect on the average Nusselt number for Richardson numbers greater than 5. Finally, Figure 9 depicts the effect of changing the rotation speed direction on the average Nusselt number. For all values of the Richardson number, the CW-CW scenario has a larger average Nusselt number than the CCW-CW scenario. This is owing to the CW-CW case having a thinner thermal boundary layer than the CCW-CW case. The effect of varying the location of the cylinders on the streamlines, isotherms, and average Nusselt number is depicted in Figures 10 and 11.

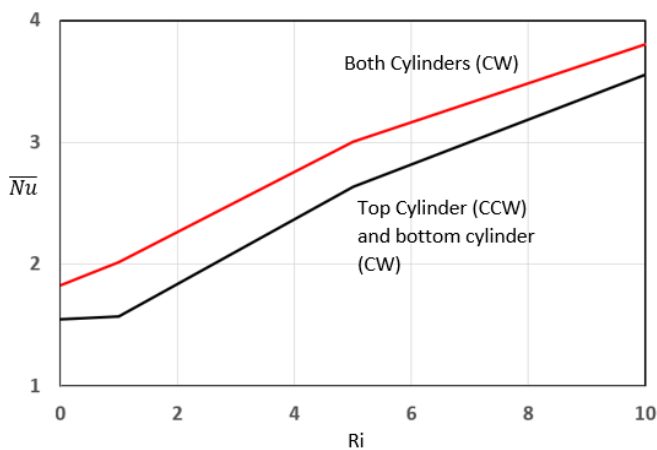


Figure 9. Effect of varying the angular velocity and Richardson number on the average Nusselt number of the top surface for different directions of cylinder angular velocity ($Re=100$, $Da=0.01$, $\omega=10$)

Figure 10 shows the effect of changing the Richardson number on the isotherms and streamlines for two cylinders placed horizontally and rotate clockwise. It can be seen from this figure that the pattern of isotherms and streamlines depends strongly on the location and spinning direction of the cylinders compared with vertical scenario. This figure illustrates that the isotherms change significantly with an increase in the Richardson number. The isotherms between the two rotating cylinders change from horizontal to inclined

shape for high Richardson numbers and this is attributed to dominant free convection compared with forced convection exhibited by the rotation of the cylinders. It is also interesting to notice from Figure 10 the existence of a small vortex near the lower right corner of the trapezoid at high Richardson numbers. Finally, Figure 11 demonstrated a comparison of the average Nusselt number between two scenarios. It can be seen from this figure that the average Nusselt number increases with an increase in Richardson number. Also, it was found the average Nusselt number is higher when placing the cylinders vertically and rotating clockwise compared with horizontal scenario.

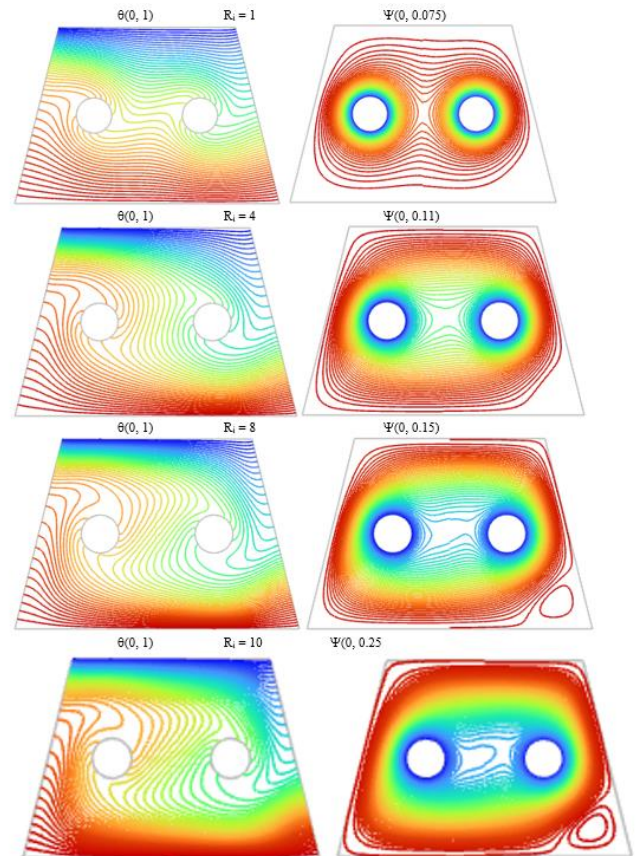


Figure 10. Effect of varying the Richardson number on the streamlines and isotherms for two cylinders placing horizontally and rotating CW ($Re=100$, $Da=0.01$, $\omega=10$)

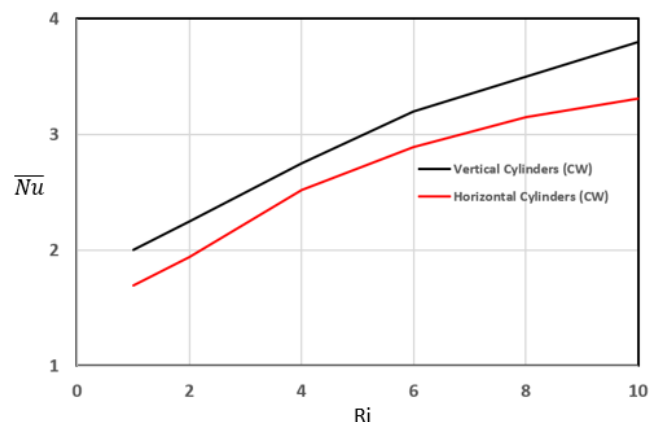


Figure 11. Effect of varying the Richardson number on the average Nusselt number of the top surface for different locations of the cylinders ($Re=100$, $Da=0.01$, $\omega=10$)

4. CONCLUSIONS

For varied Richardson numbers and rotation speeds, the effect of two revolving cylinders on the flow and heat transfer processes inside a trapezoidal enclosure heated from below was numerically investigated in this experiment. The streamlines and isotherms patterns were discovered to be dependent on the Richardson number, speed rotation, and location of the cylinders in this investigation. With raising both the Richardson number and the angular speed of the cylinders, the average Nusselt number increased. The speed of the cylinders had little effect on the average Nu when the Richardson number was high. Furthermore, the results of this study revealed that for various Richardson numbers, the CW-CW case had a higher average Nusselt number than the CCW-CW case when placed vertically. Moreover, CW-CW vertical scenario exhibited higher average Nusselt number compared to CW-CW horizontal scenario.

ACKNOWLEDGMENT

This work is supported by the research sector at Kuwait University (Grant number: EM04/20).

REFERENCES

[1] Khanafer, K., Vafai, K. (2002). Double-diffusive mixed convection in a lid-driven enclosure filled with a fluid-saturated porous medium. *Numerical Heat Transfer: Part A: Applications*, 42(5): 465-486. <https://doi.org/10.1080/10407780290059657>

[2] Khanafer, K.M., Al-Amiri, A.M., Pop, I. (2007). Numerical simulation of unsteady mixed convection in a driven cavity using an externally excited sliding lid. *European Journal of Mechanics-B/Fluids*, 26(5): 669-687. <https://doi.org/10.1016/j.euromechflu.2006.06.006>

[3] Iwatsu, R., Hyun, J. M., Kuwahara, K. (1993). Mixed convection in a driven cavity with a stable vertical temperature gradient. *International Journal of Heat and Mass Transfer*, 36(6): 1601-1608. [https://doi.org/10.1016/S0017-9310\(05\)80069-9](https://doi.org/10.1016/S0017-9310(05)80069-9)

[4] Al-Amiri, A., Khanafer, K., Bull, J., Pop, I. (2007). Effect of sinusoidal wavy bottom surface on mixed convection heat transfer in a lid-driven cavity. *International Journal of Heat and Mass Transfer*, 50(9-10): 1771-1780. <https://doi.org/10.1016/j.ijheatmasstransfer.2006.10.008>

[5] Al-Amiri, A., Khanafer, K. (2011). Fluid-structure interaction analysis of mixed convection heat transfer in a lid-driven cavity with a flexible bottom wall. *International Journal of Heat and Mass Transfer*, 54(17-18): 3826-3836. <https://doi.org/10.1016/j.ijheatmasstransfer.2011.04.047>

[6] Bagai, S., Kumar, M., Patel, A. (2021). Mixed convection in a two-sided and four-sided lid-driven square porous cavity. *International Journal of Heat and Technology*, 39(3): 711-726. <http://dx.doi.org/10.18280/ijht.390305>

[7] Khalaf, A.F., Basem, A., Hussein, H.Q., Jasim, A.K., Hammoodi, K.A., Al-Tajer, A.M., Omer, I., Flayyih, M.A. (2022). Improvement of Heat Transfer by Using Porous Media, Nanofluid, and Fins: A Review.

International Journal of Heat and Technology, 40(2): 497-521. <https://doi.org/10.18280/ijht.400218>

[8] Park, Y.G., Yoon, H.S., Ha, M.Y. (2012). Natural convection in square enclosure with hot and cold cylinders at different vertical locations. *International Journal of Heat and Mass Transfer*, 55(25-26): 7911-7925. <https://doi.org/10.1016/j.ijheatmasstransfer.2012.08.012>

[9] Park, Y.G., Ha, M.Y., Choi, C., Park, J. (2014). Natural convection in a square enclosure with two inner circular cylinders positioned at different vertical locations. *International Journal of Heat and Mass Transfer*, 77: 501-518. <https://doi.org/10.1016/j.ijheatmasstransfer.2014.05.041>

[10] Park, Y.G., Ha, M.Y., Yoon, H.S. (2013). Study on natural convection in a cold square enclosure with a pair of hot horizontal cylinders positioned at different vertical locations. *International Journal of Heat and Mass Transfer*, 65: 696-712. <https://doi.org/10.1016/j.ijheatmasstransfer.2013.06.059>

[11] Corcione, M. (2007). Interactive free convection from a pair of vertical tube-arrays at moderate Rayleigh numbers. *International journal of heat and mass transfer*, 50(5-6): 1061-1074. <https://doi.org/10.1016/j.ijheatmasstransfer.2006.07.034>

[12] Chae, M.S., Chung, B.J. (2011). Effect of pitch-to-diameter ratio on the natural convection heat transfer of two vertically aligned horizontal cylinders. *Chemical engineering science*, 66(21): 5321-5329. <https://doi.org/10.1016/j.ces.2011.07.021>

[13] Sadeghipour, M.S., Asheghi, M. (1994). Free convection heat transfer from arrays of vertically separated horizontal cylinders at low Rayleigh numbers. *International journal of heat and mass transfer*, 37(1): 103-109. [https://doi.org/10.1016/0017-9310\(94\)90165-1](https://doi.org/10.1016/0017-9310(94)90165-1)

[14] Warrington, R.O., Powe, R.E. (1985). The heat transfer of heat by natural convection between bodies and their enclosures. *International Journal of Heat and Mass Transfer*, 28(2): 319-330.

[15] Chatterjee, D., Halder, P. (2014). MHD mixed convective transport in square enclosure with two rotating circular cylinders. *Numerical Heat Transfer, Part A: Applications*, 65(8): 802-824. <https://doi.org/10.1080/10407782.2013.846687>

[16] Selimefendigil, F., Öztop, H.F. (2015). Mixed convection of ferrofluids in a lid driven cavity with two rotating cylinders. *Engineering Science and Technology, an International Journal*, 18(3): 439-451. <https://doi.org/10.1016/j.jestch.2015.03.003>

[17] Khanafer, K., Aithal, S.M., Vafai, K. (2019). Mixed convection heat transfer in a differentially heated cavity with two rotating cylinders. *International Journal of Thermal Sciences*, 135: 117-132. <https://doi.org/10.1016/j.ijthermalsci.2018.07.020>

[18] Majdi, H.S., Abdulkadhim, A., Abed, A.M. (2020). Computational fluid dynamics investigation of buoyancy driven flow between circular body and wavy enclosure filled with nanofluid/porous medium. *International Journal of Heat and Technology* 38: 403-417.

[19] Al-Azmi, B.A. (2011). Natural Convection in a Trapezoidal Enclosure Filled with a Non-Darcian Porous Medium. *Journal of Porous Media*, 14(6): 467-480. <https://doi.org/10.1615/JPorMedia.v14.i6.10>

[20] Alazmi, B., Vafai, K. (2002). Constant wall heat flux

- boundary conditions in porous media under local thermal non-equilibrium conditions. *International Journal of Heat and Mass Transfer*, 45(15): 3071-3087. [https://doi.org/10.1016/S0017-9310\(02\)00044-3](https://doi.org/10.1016/S0017-9310(02)00044-3)
- [21] Alazmi, B., Vafai, K. (2004). Analysis of variable porosity, thermal dispersion, and local thermal nonequilibrium on free surface flows through porous media. *J. Heat Transfer*, 126(3): 389-399. <https://doi.org/10.1115/1.1723470>
- [22] Khanafer, K., Aithal, S.M. (2017). Mixed convection heat transfer in a lid-driven cavity with a rotating circular cylinder. *International Communications in Heat and Mass Transfer*, 86: 131-142. <https://doi.org/10.1016/j.icheatmasstransfer.2017.05.025>
- [23] Khanafer, K.M., Chamkha, A.J. (1999). Mixed convection flow in a lid-driven enclosure filled with a fluid-saturated porous medium. *International Journal of Heat and Mass Transfer*, 42(13): 2465-2481. [https://doi.org/10.1016/S0017-9310\(98\)00227-0](https://doi.org/10.1016/S0017-9310(98)00227-0)

NOMENCLATURE

C_F	Forchheimer coefficient
Da	Darcy number
H	Height of the cavity

k	Thermal conductivity
g	Gravitational acceleration
Gr	Grashof number
p	Pressure
Pr	Prandtl number
r	Radius of the cylinder
Re	Reynolds number
T	Temperature
U, V	Nondimensional velocity in X and Y directions
X, Y	Nondimensional coordinates

Greek symbols

α	thermal diffusivity, $m^2 \cdot s^{-1}$
β	thermal expansion coefficient, K^{-1}
ε	Porosity
θ	Nondimensional temperature
ν	kinematic viscosity
ω	Nondimensional angular velocity

Subscripts

<i>c</i>	Cold
<i>eff</i>	Effective
<i>f</i>	Fluid
<i>h</i>	Hot
<i>s</i>	Solid